JOURNAL OF GEOPHYSICAL RESEARCH, VOL. 103, NO. A2, PAGES 2219–2229, FEBRUARY 1, 1998

Further investigation of auroral roar fine structure

S. G. Shepherd, J. LaBelle, and M. L. Trimpi

Department of Physics and Astronomy, Dartmouth College, Hanover, New Hampshire

Abstract. In April 1996, a downconverting receiver was operated in Churchill, Manitoba, Canada, to increase the statistics about the recently discovered fine structure of auroral roar emissions. Auroral roar is found to be both structured and unstructured. A wide variety of previously unknown tonal features drifting in a complicated manner were recorded. These structured features can be classified according to their duration, frequency drift, and grouping with like features. Typically, 95% of the structured features last less than 1 s. The slope of drifting features is more commonly negative than positive with a magnitude typically less than a few kHz s^{-1} and a maximum of $\sim$ 800 kHz s^{-1}. The minimum bandwidth of features is 6 Hz or less, and typical separation between similar features is $\sim$ 400 Hz. These measurements form a basis for reviewing proposed generation mechanisms of auroral roar including a localized source model and laser cavity mechanism.

1. Introduction

The auroral ionosphere is a natural emitter of radio waves, and many of these emissions are observable at ground level. Several types of radio emissions have been well documented using a variety of ground-based, stepped-frequency receivers (see reviews by *LaBelle* [1989] and *LaBelle and Weatherwax* [1992]). In particular, auroral roar is a relatively narrowband emission at roughly 2 and 3 times the local electron cyclotron frequency (f_{ce}) [*Kellogg and Monson*, 1979, 1984; *Weatherwax et al.*, 1993, 1995]. Much effort has been made in characterizing the seasonal, diurnal, and spectral characteristics of auroral roar to aid in determining its generation mechanism [e.g., *Weatherwax et al.*, 1995].

LaBelle et al. [1995] report two auroral roar events measured in September and October 1994, with a downconverting receiver operated in a semiautomatic mode in Circle Hot Springs, Alaska. These recordings revealed for the first time that auroral roar is composed of multiple narrowband features previously unresolved by stepped-frequency receivers. These initial examples showed the lower bound of the bandwidth of some individual features to be about 30 Hz. Both rising tones and falling tones were observed, and the slopes of the discrete features varied from +1 to −100 kHz s^{-1}. The discrete features occurred in groups often spaced as close as several hundred hertz. The peak power spectral density of individual features was 1–2 $\times 10^{-13}$ V^2 m^{-2} Hz^{-1} [*LaBelle et al.*, 1995].

Paper number 97JA03171.
0148-0227/98/97JA-03171$09.00

To increase the number of examples of auroral roar fine structure, we operated the same downconverting receiver at the Northern Studies Centre in Churchill, Manitoba, Canada, during a 3-week campaign in April 1996. One of us (S.G.S.) controlled the center frequency of the downconverter according to information provided by a collocated swept-frequency receiver. The goal of this campaign, based on the two events from 1994, was to collect numerous examples of auroral roar fine structure so we could perform statistical studies of duration and drift of individual features. Presented below are an instrumentation section discussing the radio receivers used in the campaign, a data section showing the auroral roar fine structure captured, a classification scheme for the variety of features observed, and, finally, an interpretation section where the data are interpreted in terms of the two generation mechanisms that have appeared in the literature.

2. Instrumentation

Several types of radio receivers have been developed at Dartmouth College and deployed in the auroral zones. Two such receivers were used during this campaign to investigate roar fine structure: a programmable stepped-frequency receiver (PSFR) and a tunable downconverting receiver (DCR).

The PSFR, described elsewhere [e.g., *Weatherwax*, 1994], is a versatile receiver tuned by a personal computer which also records the receiver output. The PSFR sweeps 0.03–5.00 MHz every 2 s in 10-kHz steps. Since November 1991, Dartmouth has operated a PSFR at Churchill in a semiautomatic manner in which data are collected, digitized, and stored by the computer and sent back to us on a biweekly basis. Churchill is located

at 58.76°N, 265.92°E, and 69.2° invariant latitude, and midnight magnetic local time occurs at 0635 UT.

The tunable DCR translates the received signal to base band allowing the output to be recorded on standard 90-min audio cassette tapes with ~12-kHz bandwidth. The operator may tune the DCR to any desired 10-kHz band between 10 kHz and 5 MHz. Audio output from the DCR in conjunction with the real-time visual display of the output of the PSFR was used to tune the DCR. So that events could be matched from the two receivers, audio time stamps from the PSFR were mixed with the DCR output signal and recorded onto the cassette tapes every minute. In addition, the DCR was equipped with a microphone so voice announcements about the tuning of the DCR and notes on the visible aurora could be recorded.

The campaign window was chosen to occur near the equinox and during a peak in the geomagnetic activity as measured by the Kp index because previous studies have shown that occurrences of auroral roar tend to maximize at these times [*Weatherwax et al.*, 1995]. During the entire campaign the PSFR operated for 20 hours per day centered on local midnight (0600 UT). DCR recordings of radio emissions were made for 19 nights between March 30 and April 17. On a typical night, observing began at ~ 1900 LT (0100 UT) and ended near local midnight (0600 UT) unless roar was observed after ~ 2300 LT in which case the observing

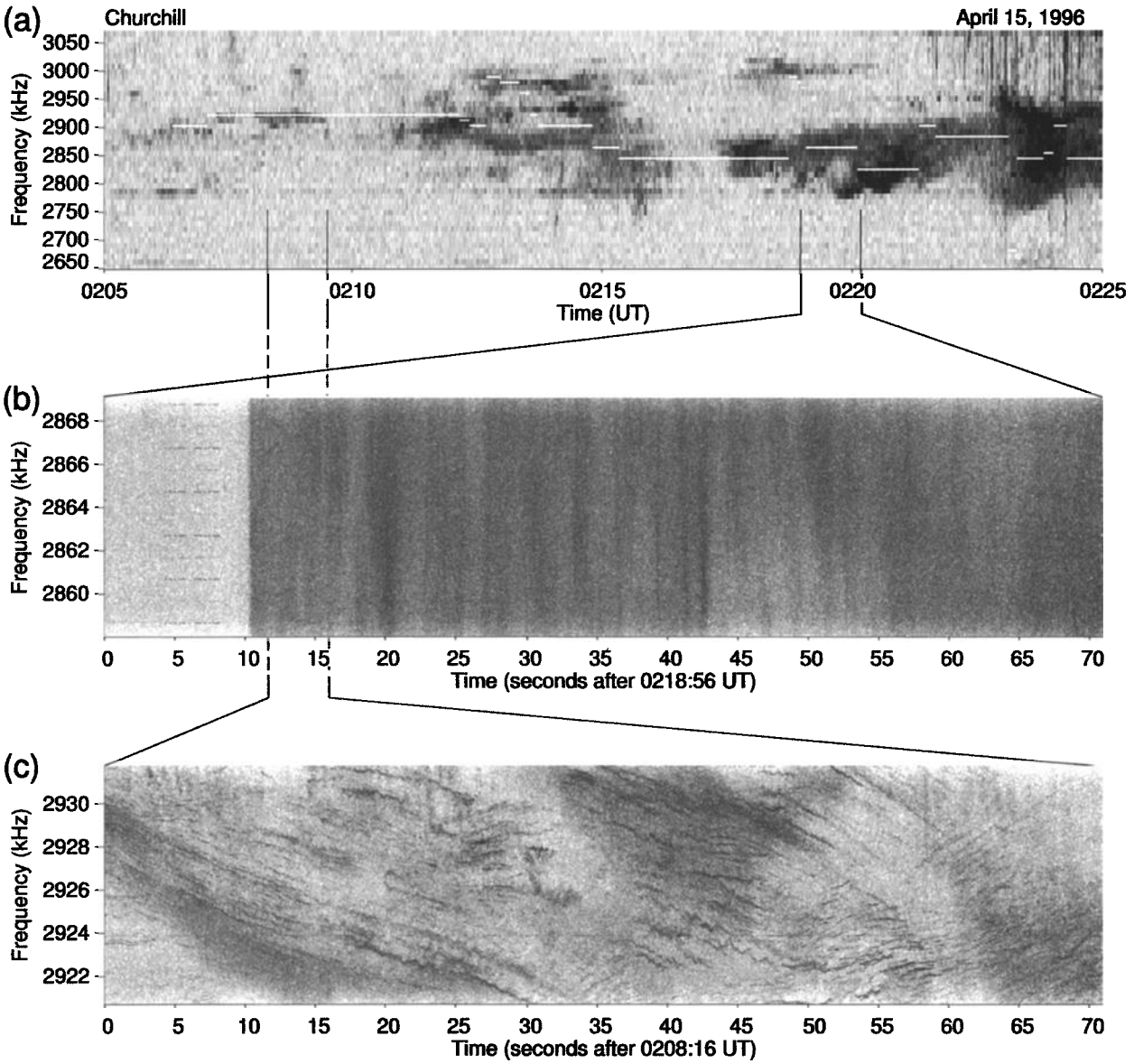

Figure 1. (a) Swept-frequency receiver spectrogram of an auroral roar event, recorded at Churchill, Manitoba, Canada, on April 15, 1996, which was also captured with the tunable down-converting receiver (DCR). The white line indicates the center frequency of the DCR, and vertical lines indicate the start of the records shown below, which illustrate: (b) unstructured and (c) structured auroral roar fine structure.

window was extended until quiet radio conditions existed for a full hour. When auroral roar was detected with the PSFR, the DCR cassette tape was started, and the DCR was tuned to the desired frequency. The audio output of the DCR allowed interesting portions of the auroral roar to be sampled. During prolonged periods of radio quiet the tape was stopped, but often the tape was left recording during these quiet periods between roar to capture the onset of some events. In addition, after the normal observing hours the DCR was set to a likely frequency and left to run in automatic mode for 90 min each night.

Auroral roar was recorded on 11 of the 19 nights of observation. Of 36 audio cassettes recorded in the field, 17 contain auroral roar events for an estimated 600 min of total event time. Thus the campaign was successful in increasing by several orders of magnitude the quantity of high-time and high-frequency resolution auroral roar data. The data revealed a much greater variety of fine structure features than had been recorded previously.

3. Observations

At Dartmouth the audio cassettes were played back into a computer from a standard tape deck through a postemphasis analog filter to restore the signal response. A prerecording deemphasis was used to avoid tape saturation at high frequencies, caused by the normal audio preemphasis. The system then provides a flat response up to 12 kHz with added dynamic range at high frequencies at the expense of a poorer signal to noise ratio. A 32-kHz sample rate was used to digitize the analog tapes. Survey sonograms of the digitized data were made for each cassette tape. Furthermore, the resulting large digital data files were split into 20-Mb sections containing roughly 5 min (312.5 s) of data each, and more detailed survey plots of these files were created to look for interesting events. From these survey plots, interesting times were selected. Owing to the large quantity of data, only the most interesting tapes were processed based on notes made during the recordings while at Churchill, resulting in ~600 min of digitized data.

From this initial survey it became apparent that a major classification could be made based on the appearance of the fine structure. That is, the auroral roar, when viewed at high-time and high-frequency resolution, falls into one of two broad categories: structured or unstructured. An unstructured event appears as a uniform enhancement of noise, although sometimes it appears patchy in time and/or frequency. No amount of frequency or temporal magnification can resolve spectral features. Structured events contain at least some spectral and temporal features which distinguish them from noise or unstructured events.

Figure 1a shows a spectrogram of an auroral roar recorded during the campaign with the PSFR. The horizontal white lines running through Figure 1a indicate the frequency setttings of the DCR. The bandwidth of the DCR is roughly the vertical width of the PSFR pixel. Figure 1b shows DCR output starting at 0218:56 UT as indicated by the second set of vertical lines in Figure 1a. Figure 1b illustrates an example of unstructured roar fine structure. The record begins at a time of relative radio quiet at 2.97 MHz and then switches into unstructured roar at 2.86 MHz 10 s into the record. Figure 1c shows DCR output starting at 0208:16 UT as indicated by the first set of vertical lines in Figure 1a. Figure 1c shows an example of structured roar. This example illustrates that auroral roar is often composed of many different types of features: rising, falling, stationary, wavy, short, and long.

In a random survey of a subset of the digitized data, 18 1-min intervals contained structured auroral roar while 12 of these 18 intervals also contained unstructured roar. Nowhere in this survey did unstructured roar occur without at least one structured feature. In somewhat rare circumstances, roar can be unstructured but patchy in nature as opposed to the more common broadband phenomena in which the entire ~12-kHz bandwidth of the DCR contains no structure.

Structured auroral roar comprises many spectral and temporal features as shown in Figures 2a-2h. These examples were chosen from expanded survey plots to show a particular spectral or temporal feature. Each frame contains 3 s and 11 kHz of DCR data displayed at identical contrast levels to aid in distinguishing different types of features. Note that the center frequencies are not identical in all plots.

The structured features can be classified according to their duration, frequency drift, and grouping with like features. Within these classifications a nearly continuous spectrum of features were recorded.

The duration of a particular spectral feature is an obvious distinction. The time durations range over 3 orders of magnitude from the minimum measurable limit of tens of milliseconds to tens of seconds. Features lasting tens of seconds, a few seconds, roughly a second, hundreds of milliseconds, and tens of milliseconds are shown in Figures 1c, 2c, 2f, 2b, and 2a, respectively.

To quantify the distribution of durations of these features, a random subset of the digitized recordings was surveyed and analyzed. The study set consisted of 18 1-min intervals. Each of these intervals was plotted at several different time and frequency resolutions to ensure that all features present were identified. The durations of features were then scaled from these plots. One to ~40 features were measured during each interval based on the number of features present. The resulting data set, consisting of ~400 time duration measurements, is shown in Figure 3 as a histogram. Figure 3a shows the number of features observed as a function of duration on a linear scale grouped into 50-ms bins, while 3b shows the same data on a logarithmic scale grouped into 0.1-dB bins. Figure 3 shows that roughly 95% of the features last less than 1 s, 3% between 1 and 2 s, and 2% last longer than 2 s.

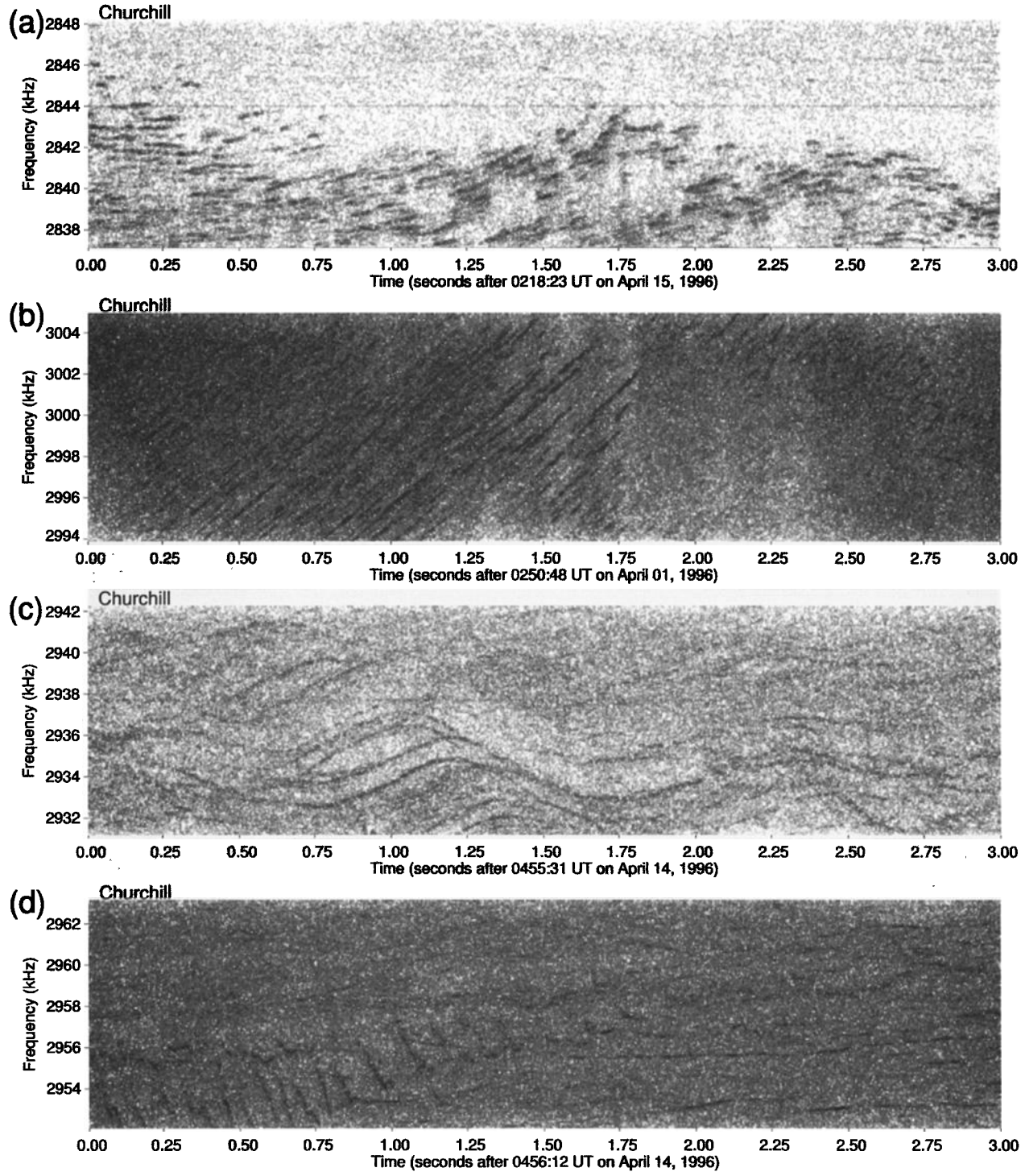

Figure 2. Three-second spectrograms showing various auroral roar fine structure features, recorded at Churchill, Manitoba, Canada: seconds after (a) 0218:23 UT on April 15, 1996, (b) 0250:48 UT on April 1, 1996, (c) 0455:31 UT on April 14, 1996, (d) 0456:12 UT on April 14, 1996, (e) 0307:22 UT on April 11, 1996, (f) 0323:01 UT on April 09, 1996, (g) 0504:01 UT on April 14, 1996, (h) 0311:24 on April 11, 1996.

The spikes in the log distribution near the lower limit (-1.5 and -1.8) are most likely a result of quantization error due to the resolution of the measurement technique. In reality, these spikes are dispersed into the adjacent gaps giving a more uniform distribution which rolls off below -1.5 ($\sim$0.03 s) at the low end. The apparent lower limit near -2.0 (10 ms) is due to the bandwidth of the signals which require at least a $\sim$10-ms fast

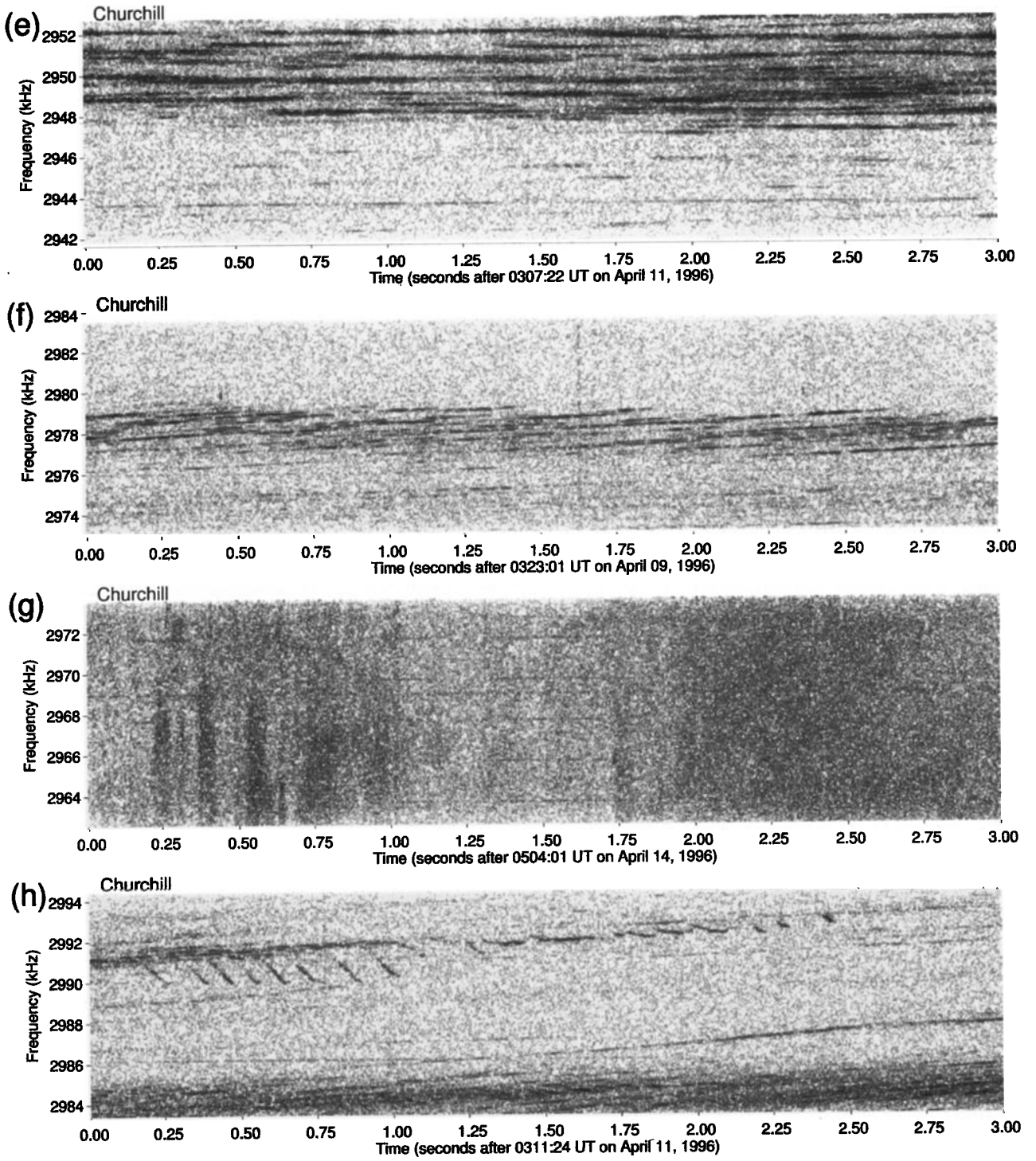

Figure 2. (continued)

Fourier transform (FFT) for sufficient resolution to be identified. It cannot be excluded that features of shorter duration exist.

The apparent upper cutoff in the distribution is somewhat exagerated in part because features tend to drift through the bandwidth of the DCR and as a result are truncated in duration. In addition, the length of the random survey plots (1 min) may have truncated longer features. Also, the difficulties in predicting at what frequency roar would occur forced the operator to tune into the frequency band of an ongoing roar thus shortening some features. Perhaps the most influential aspect of the subjectivity involved in the time duration survey is the contrast level of the survey plots. It was necessary to adjust the contrast on some survey plots to discern the features from the noise. In some cases the intens-

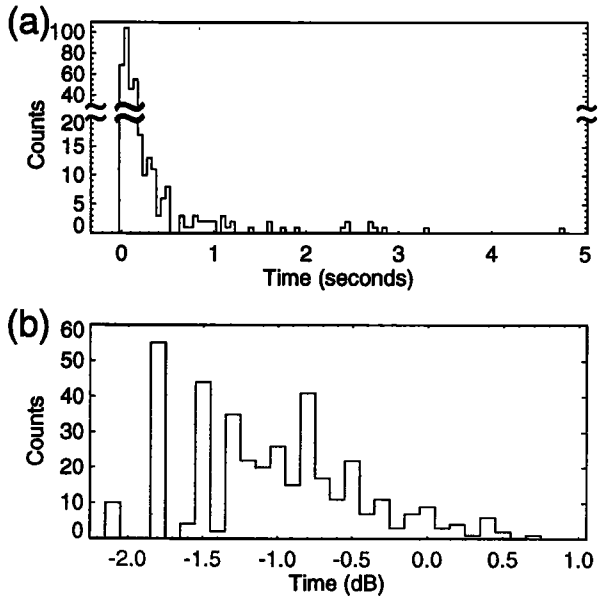

Figure 3. The durations of fine structure features in a survey of structured events. The duration ranges from the instrumental limit of ~10 ms to several seconds. (a) Linear scale. (b) Logarithmic scale.

ity of a particular feature appeared to be intermittent thus making it difficult to judge whether a feature was, indeed, a single event or several. Despite these experimental difficulties the data establish that the majority of auroral roar fine structure features are typically less than a few seconds in duration and predominantly less than 1 s.

Another characteristic feature is the frequency drift of fine structures. Figure 2c shows features which drift in a variable manner that is nearly sinusoidal. Other variable drifting features are shown in Figure 1c and Figure 4. Many groups are composed of individual features with a constant frequency drift. For example, Figures 2b and 2f show constant upward slopes, Figures 2d and 2h show constant downward slopes, and Figure 2e shows constant zero slopes.

The features with constant drifts vary greatly from ~-800 kHz s^{-1} to ~+100 kHz s^{-1}. Figures 2b, 2d, and 2h illustrate features with extreme frequency drift magnitudes > 10 kHz s^{-1}, Figures 2a, 2d, 2f, and 2h show features with more moderate drift magnitudes < 10 kHz s^{-1}, and Figures 2a and 2f depict roughly stationary features that drift very little. It became apparent from inspection of the survey plots that the slope of extremely steep drifting features is much more commonly negative than positive. To quantify this observation, the initial ~5-min survey plots were carefully analyzed for features with constant drifts, in particular those with drift magnitudes >~10 kHz s^{-1}. The slopes of features were not randomly selected in order to ensure that we included the largest observed drifts. In this survey all features with drifts exceeding ~ ±10 kHz s^{-1} were measured, but for lesser slopes only a few representative events were measured.

Figure 5 shows a histogram of the number of features with constant drifts versus frequency drift. Because only a few representative features were measured from the large number of slopes <~10 kHz s^{-1} in magnitude, the middle of the distribution is undersampled. The negative drift tail in the distribution in Figure 5 is longer than the positive drift side, supporting the notion that more negative steeply drifting features exist and that the steepest tend to be negative. Of the 139 features measured with slopes > 10 kHz s^{-1} in magnitude, 107 were negative, and the largest negative and positive slopes observed were -790 kHz s^{-1} and +88 kHz s^{-1}, respectively.

Solitary features, those occurring by themselves during a time much longer than the feature duration, are observed in less than 1% of the structured examples of the digitized data. Features more often occur in groups with similar characteristics. These groups contain up to several hundred features. Figures 2h and 2c show groups containing several like features, Figures 2b, 2e, and 2f show groups with many more features, and Figure 2a shows a group with nearly 100 within 3 s. The spacing of individual features in the 18 random 1-min sur-

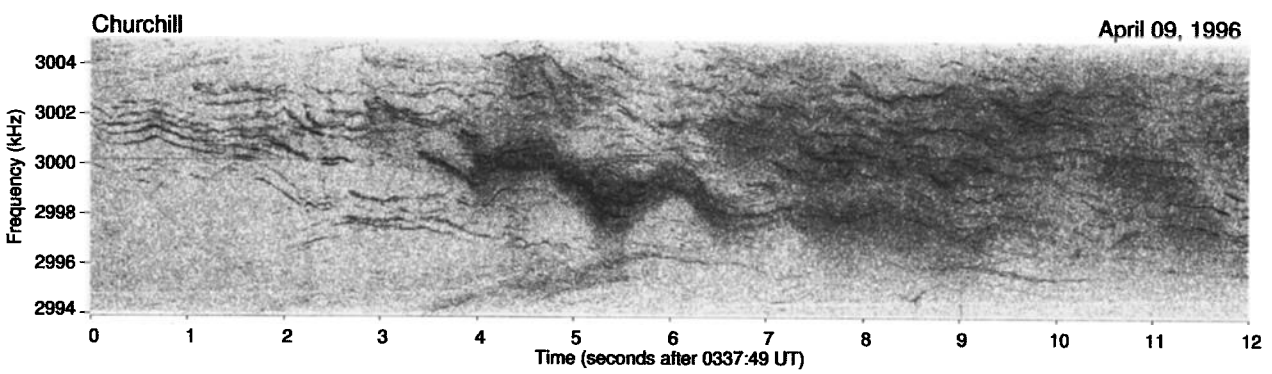

Figure 4. Auroral roar fine structure, recorded at Churchill, Manitoba, Canada, on April 9, 1996, which contains four to five multiplet features at the beginning of the record near 3 MHz, many other examples of multiplets, and intensity pulsations of ~1 Hz beginning 4 s into the record.

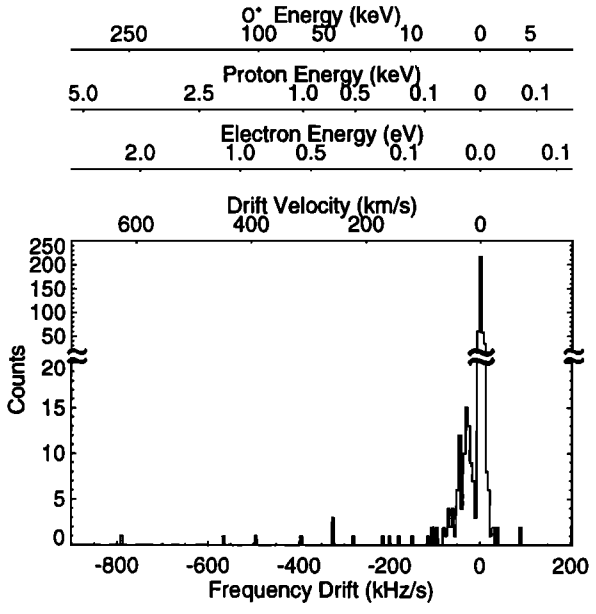

Figure 5. The frequency drifts of fine structure features in a survey of a subset of structured events. Typical drifts are < 10 kHz s^{-1}, but values as large as -790 kHz s^{-1} and +100 kHz s^{-1} occur. The largest drifts are predominantly negative (frequency decreasing with time).

vey plots ranges from ~150 Hz to several kilohertz with most of the features spaced closer than 1 kHz. The median spacing of these features is ~450 Hz. Figures 2a-2f, 2h, and 4 show at least some features spaced closer than 1 kHz.

The minimum bandwidth of auroral roar fine structure is an important clue in determining the generation mechanism. Any model proposed must provide explanations for the coherence of the emissions. Some mechanisms may be elimated on the basis that they provide no feasible explanation of the observed fine structure. To improve the upper bound of the minimum bandwidth of roar fine structure, it is necessary to analyze stationary features. Figure 6a is a spectogram showing several relatively stationary features observed at 0207:23 UT on April 15. In particular, the feature beginning 2 s into the record and highlighted with a box is stationary in frequency for roughly 1 s. The inset in Figure 6b shows a series of spectra each of which represents a 0.256 second FFT, implying a full width at -3 dB of ~5.5-Hz resolution. The measured bandwidth of 6 Hz is the resolution limit of the FFT. The actual bandwidth of the signal may be less than 6 Hz but not greater.

Difficulties in locating a feature which remains stationary for long enough to give better frequency resolution prevent further refinement of the minimum bandwidth. Tape flutter and wow in the recording equipment are ~ 5 Hz which prevents further refinement even if more stationary features are found thus allowing longer FFTs. However, a new digital DCR is being designed which addresses these difficulties.

4. Interpretation

Two competing mechanisms have been proposed to explain the generation of auroral roar emissions in the ionosphere: direct excitation of X mode electromagnetic waves by the auroral electrons via the cyclotron maser instability [*Weatherwax et al.*, 1995; *Yoon et al.*, 1996] and generation of electrostatic upper hybrid waves at altitudes where $f_{uh} = nf_{ce}$, followed by conversion of these waves to electromagnetic waves via one of several linear and nonlinear mechanisms [e.g., *Gough and Urban*, 1983; *Weatherwax et al.*, 1995]. Recently, *Yoon et al.* [1998] present a unified model of these mechanisms, showing that for auroral parameters the growth rate of the electrostatic upper hybrid waves is 2–3 orders of magnitude greater than that of the cyclotron maser stimulated X mode waves; however, the efficiency with which the upper hybrid waves convert to electromagnetic radiation remains an open question.

Both of the candidate generation mechanisms predict that the frequency of the excited waves nearly equals 2 or 3 times the local electron gyrofrequency. This condition implies that the observed frequency of the emission is related to the source altitude, and the frequency drift of the emissions is related to the motion of the source. For a dipole magnetic field the component of the source velocity along the field is given by [e.g., *Gurnett and Anderson*, 1981; *LaBelle et al.*, 1995]:

$$\frac{dr}{dt} = -\frac{R_E}{3}\left(\frac{nf_0}{f^4}\right)^{1/3}\frac{df}{dt} \quad (1)$$

where f_0 is the electron gyrofrequency at ground level, $f = nf_{ce}$ is the emission frequency, and R_E is the radius of the Earth. For parameters typical of auroral roar observations (f_0 = 1.6 MHz and f = 2.8 MHz) [*Weatherwax et al.*, 1995], (1) can be simplified to $dr/dt \cong -0.79df/dt$, where the spatial variation is given in kilometers and frequency is given in kilohertz.

Using this relation, the maximum observed frequency drift (-790 kHz s^{-1}) corresponds to a source moving upward at ~620 km s^{-1}, and typical observed frequency drifts (±0–10 kHz s^{-1}) correspond to source motions upward and downward of magnitude 0–800 m s^{-1}. For comparison, at F region altitudes the ion sound speed is typically 1.4–2.5 km s^{-1} assuming that O^+ is the dominant ion, and the Alfvén speed is about 900 km s^{-1}. The drift velocity estimated from the maximum observed frequency drift measured approaches that of the local Alfvén speed, but typical drift velocities < 10 km s^{-1} are closer to the ion sound speed. The thermal velocities of 10 keV oxygen ions, 100 eV protons, and 0.1 eV electrons also fall in the range of observed source velocities, as shown in Figure 5.

Assuming generation of the auroral roar fine structures at locations where $f = 2f_{ce}$ in a dipole field, the separation of fine structure features by 100–1000 Hz implies source regions vertically separated by a few hundred meters. The upper bound on the minimum band-

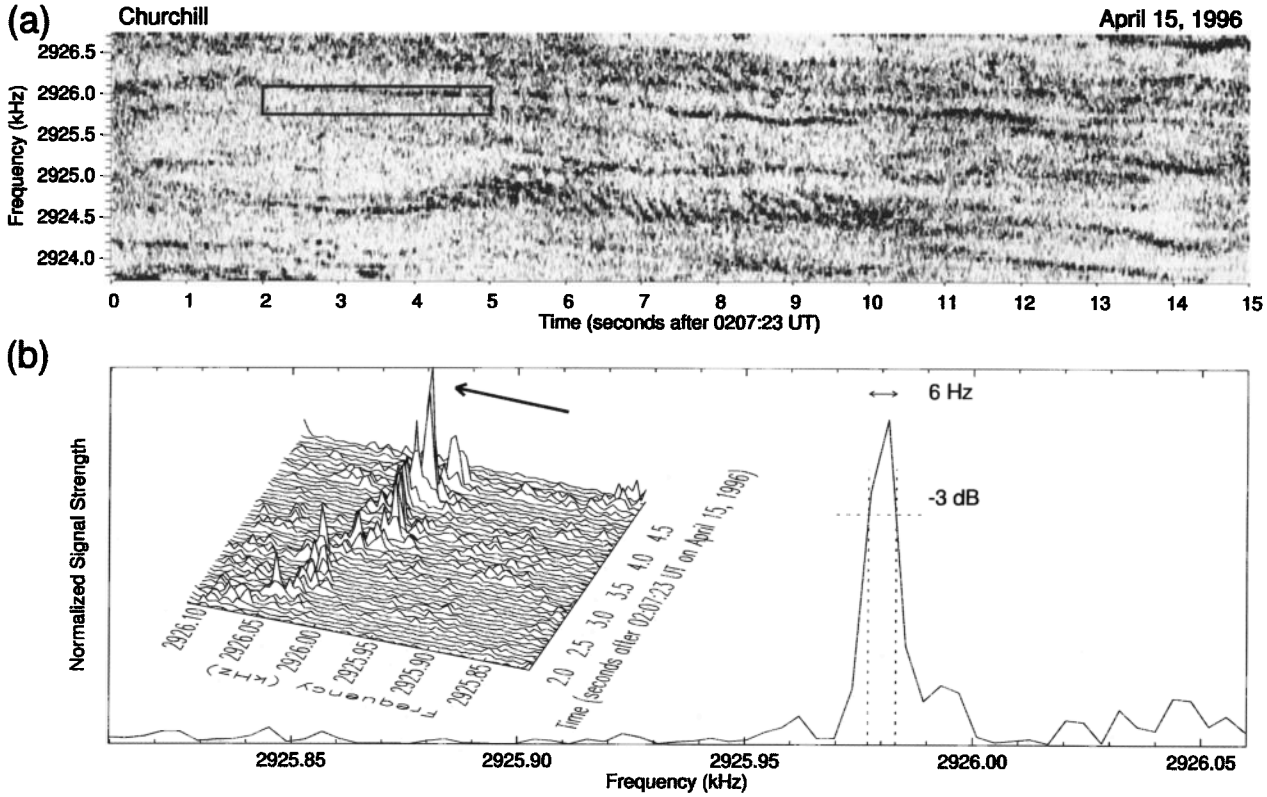

Figure 6. (a) A relatively stationary auroral roar fine structure feature (boxed) used for determining the minimum bandwidth of auroral roar fine structure features, recorded at Churchill, Manitoba, Canada, on April 15, 1996. The boxed spectra in Figure 6a are shown in the (b) hidden-line plot which also displays the individual spectrum noted by the arrow in the inset. The minimum bandwidth is ~6 Hz, limited by the fast Fourier transform and not the signal.

width of 6 Hz restricts the vertical spatial extent of the source to as small as a few meters, 2 orders of magnitude less than the free space wavelength at $f = 2.9$ MHz. The effective $Q \equiv f/\delta f$ of the emission process is 5×10^5.

Two other observed emissions, auroral kilometric radiation (AKR) and Jovian decametric S bursts, also exhibit fine structure. Table 1 summarizes some charateristics of these emissions for comparison to the less well known auroral roar.

AKR exhibits fine structure strikingly similar to that of auroral roar. As in auroral roar, both upward and downward drifting features are observed, and the ve-

Table 1. Comparision of Auroral Roar, AKR, and Jovian Decametric S Burst Emissions

	Auroral Roar[a]	AKR[b]	Jovian Decametric S Burst[c]	Units
Frequency of emission	2.5–3.2 ($\sim 2f_{ce}$) 3.6–4.3 ($\sim 3f_{ce}$)	.05–.7 ($\sim f_{ce}$)	3–35 ($\sim f_{ce}$)	megahertz
Source altitude	26υ–60υ km	0.3–2.3 R_E	~0.01–0.28 R_J [d]	
Power	1–10	10^9	10^{10}	watts
Observed polarization	left	right or left	right or left[e]	elliptical
Typical feature duration	< 1	~ 1	50–100 x 10^{-3}	seconds
Typical drift frequency	≤ few	few	~2x10^4	kHz s^{-1}
Typical feature separation	≥ 400	10^4	...	hertz
Minimum bandwidth	≤ 6	5	< 2x10^{3}[f]	hertz

[a] [*Weatherwax et al.*, 1993; *LaBelle et al.*, 1995; *Shepherd et al.*, 1997].
[b] [*Baumback and Calvert*, 1987; *Calvert*, 1982; *Gurnett and Anderson*, 1981].
[c] [*Warwick et al.*, 1979; *Ellis*, 1980, 1982; *Zarka et al.*, 1996].
[d] 17 MHz.
[e] Hemisphere dependant.
[f] *Zarka et al.* [1996] states ≤ 20 x 10^3.

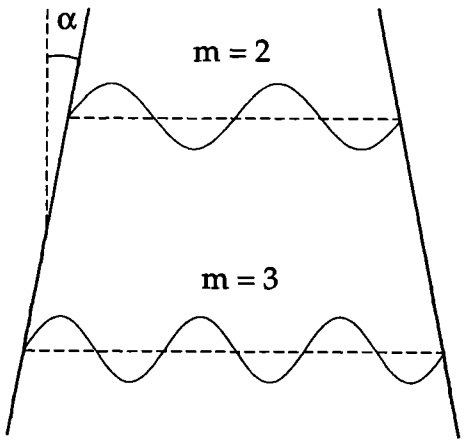

Figure 7. A model of an ionospheric density cavity in which waves reflect at the cavity walls such that an integer number of wavelengths fit in the cavity. Two adjacent feedback paths are shown with waves containing two and three wavelengths. The walls of the cavity make an angle α with the vertical. The wave along the lower altitude feedback path has a shorter wavelength because of the stronger magnetic field. Adjacent feedback paths are possible with vertical walls ($\alpha = 0$), but the vertical separation between paths, and hence frequency separation, is reduced by vertically converging walls ($\alpha > 0$).

locities inferred from these drifts assuming generation at $f = f_{ce}$ are generally comparable to the sound speed and are much less than the Alfvén speed [*Gurnett and Anderson*, 1981]. Nonharmonic multiplet features such as those seen in Figure 4 are also present in AKR fine structure [*Calvert*, 1982]. As in auroral roar, the minimum bandwidths of the AKR fine structure correspond to vertical source dimensions smaller than the free space wavelength [*Baumback and Calvert*, 1987]. Of course, AKR is generated at much higher altitudes than auroral roar, and the intensity of AKR averaged over its bandwidth (of the order of 10^{-11} V^2 m^{-2} Hz^{-1} at 25 R_E) far exceeds that of auroral roar ($\sim 10^{-15}$ V^2 m^{-2} Hz^{-1} at a few hundred kilometers).

The similarities between AKR fine structure and auroral roar fine structure suggest similar mechanisms. *Calvert* [1982] explains the extremely narrow bandwidth of AKR fine structures with a laser-feedback model: the boundaries of field-aligned density depletions provide the mirrors, and the unstable electron distribution provides the energy to the waves. Excitation occurs where an integer number of wavelengths fit across the density cavity. Provided that the wave growth across the cavity is sufficient to make up for the loss upon reflection, the wave grows to saturation. The excited wave is, in principle, perfectly monochromatic with frequency determined by the cavity dimensions. As the cavity dimensions change, the frequency drifts. Both upward and downward frequency drifts are thus naturally explained. Multiplet structures arise when m, $m + 1$, $m + 2$, etc. wavelengths fit into the density cavity at various locations along the field line. In the case of AKR the cyclotron maser growth rate is so large that an effective reflection coefficient of 1% or less suffices to produce the overall unity gain required for laser action. In the *Calvert* [1982] model the bandwidths and frequency spacings of multiplet structures composing AKR can be explained based on electron density cavities that are expected to exist in the AKR source region.

Unlike the case of AKR, the cyclotron maser mechanism at ionospheric altitudes is characterized by a low growth rate [*Weatherwax et al.*, 1995; *Yoon et al.*, 1996, 1998]. Hence, if the laser-feedback mechanism is to explain the fine structure of auroral roar, the reflection coefficient at the density cavity boundaries must be of the order of 99%, which seems unlikely, especially if the cavity walls are not perpendicular to the wave path. Nevertheless, it is instructive to consider the plausibility of the laser-feedback mechanism from a purely geometric perspective. Figure 7 illustrates a density cavity with walls making an angle α with vertical. A density cavity with this geometry is realized by considering a horizontal density cavity and an upward density gradient. The result is a field-aligned cavity with vertically converging walls similar to the geometry used by *Calvert* [1982] and not uncommon in the auroral zone. Two adjacent feedback paths are illustrated: one correpsonding to two wavelengths fitting across the cavity and the other corresponding to three wavelengths. The wavelength of the waves is shorter at lower altitude paths, where the frequency is higher, and therefore it is possible to have multiplet structures even in a cavity with vertical walls ($\alpha = 0$). Assuming the X mode dispersion relation and generation of the waves in a dipole field geometry where $f = 2f_{ce}$, it is possible to evaluate the vertical

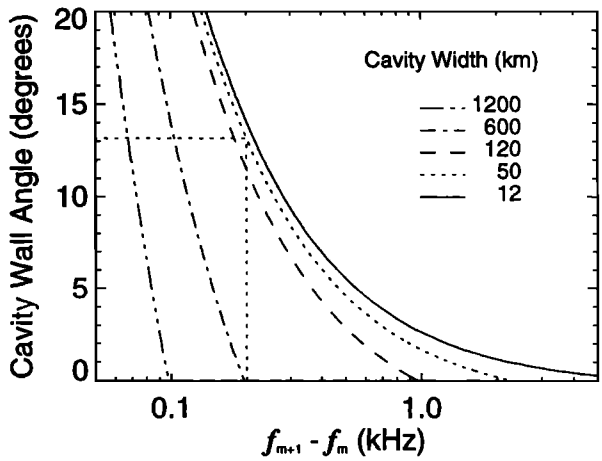

Figure 8. The angle (α) a cavity wall (as modeled in Figure 7) must make with vertical in order that adjacent feedback paths are separated by a frequency Δf is shown for cavity widths ranging from 12 to 1200 km. For reference, the dotted line indicates that for a 50-km-wide cavity the observed frequency separation between multiplets of $\sim$200 Hz (Figure 4) requires $\alpha > 13°$.

separation of adjacent feedback paths and hence the frequency spacing of the multiplet structures as a function of α. Figure 8 illustrates the result. For vertical walls ($\alpha = 0$) the observed frequency spacings of 100–500 Hz would require a density cavity with horizontal dimension $10^2 - 10^3$ km, larger than typically observed in the ionosphere. F region density structures exist on a wide range of scales, but well-defined, field-aligned cavities most commonly have scales of tens of kilometers [*Doe et al.*, 1993]. A cavity dimension of 50 km requires a cavity wall angle (α) of over 13° to explain the observed 200-Hz frequency spacings. This geometry is perhaps not out of line with observations; however, it is hard to understand how > 99% of the wave energy can be reflected back along the feedback path under this condition. Of course, the cyclotron maser instability might still be responsible for the unstructured roar, which exhibits no multiplet features, or even structured roar if an approach other than the laser-feedback one is used.

Jovian decametric radiation contains substructure such as "S bursts" which superficially resemble the fine structure in auroral roar reported here. *Ellis* [1974] proposed a mechanism for the Jovian S bursts involving radiation from electrons moving adiabatically within the Jovian magnetic field and radiating at the local cyclotron frequency. To consider whether this idea has relevance to the auroral roar fine structure emissions, following *Zarka et al.* [1996], we write an expression for the time derivative of the frequency generated by an electron moving adiabatically in a dipole magnetic field and radiating at twice the local electron cyclotron frequency:

$$\frac{df}{dt} = \frac{-3}{LR_E} g(\theta) f v \left[1 - \sin^2(\Phi_{eq}) \frac{\pi m_e f L^3}{B_{eq} e}\right]^{1/2} \quad (2)$$

where f is the wave frequency, L is the McIlwain L parameter of the field line, v is the electron's velocity, Φ_{eq} is its equatorial pitch angle, m_e is its mass, B_{eq} is the magnetic field strength at the equator at $L = 1$, θ is the magnetic colatitude, and $g(\theta)$ is a factor nearly constant and of the order of unity at auroral latitudes:

$$g(\theta) = \frac{\cos\theta}{\sin^2\theta} \frac{(3 + 5\cos^2\theta)}{(1 + 3\cos^2\theta)^{3/2}} \quad (3)$$

The observed fine structures often extend over all or most of the 10-kHz bandwidth of the receiver, which corresponds to an altitude range of about 10 km if the radiation is at the electron cyclotron harmonic in a dipole field. Even within ~ 10 km of the electron's reflection height, df/dt greatly exceeds the observed values for all except thermal electrons. For example, within 1–10 km above its reflection point a 1-keV electron with an equatorial pitch angle of 10.5° acquires a parallel velocity sufficient to make $df/dt = -200$ to -2000 kHz s^{-1}, overlapping with the upper range of the observations. To produce df/dt of the order of 10 kHz s^{-1} over a 10-kHz band requires ≤ 0.1 eV electrons. Hence only for thermal electrons is the adiabatic motion of the electrons consistent with the drifting patterns of the fine structures.

However, another problem with this hypothesis is that the time durations of the fine structures (Figure 3) generally exceed the inverse electron-neutral collision frequency, which is of the order of 10^{-3}–10^{-1} s at F region altitudes, depending on the phase of the solar cycle [*Kelley*, 1989, appendix]. If the emissions are nonthermal, they must be related to a nonthermal feature of the electron velocity distribution such as a loss cone, but for a given population of electrons such a feature will be isotropized on the timescale of the collision frequency. Since the fine structure features last much longer than the collision time, it is unlikely that they result from the adiabatic motion of an individual batch of electrons, even if for thermal electrons this motion can explain the frequency variation. The long timescale of the fine structure features relative to the collision time suggests that the fine structure frequency is selected by a condition on the wave conversion or excitation process rather than by the motion of individual electrons or batches of electrons. The frequency selection could be linked directly or indirectly to ion motion, however, as the ion collision frequency is much lower.

5. Conclusion

LaBelle et al. [1995] described initial observations of the fine structure of auroral roar emissions. Further observations described here reveal a greater variety of fine structures than suggested by the earlier observations: features that drift upward in frequency, drift downward in frequency, and drift both up and down and features with zero frequency drift and others with frequency drifts approaching 1 MHz s^{-1}. There is evidence for an asymmetry in that the largest frequency drifts are predominantly negative (frequency decreasing with time). Durations of the events range from the instrumental limit of ~ 10 ms to several seconds. When multiple structures are observed simultaneously, the frequency spacing between these is in the range 100–500 Hz. Significantly, the bandwidth of the features is in some cases less than 6 Hz ($f/\delta f \sim 5 \times 10^5$); if the source size is inferred from the $f = 2f_{ce}$ matching condition in a dipole field, its vertical extent must be smaller than the wavelength of the electromagnetic waves.

No theory addresses the generation of auroral roar fine structure. For similar fine structure in AKR, *Calvert* [1982] suggests a laser-feedback mechanism in which the walls of a density cavity feed a portion of the electromagnetic energy back into the region where electron energy is converted to waves via the cyclotron maser instability. For the X or O modes at ionospheric altitudes this idea seems implausible for a cavity with vertical (field-aligned) walls, because it requires too large a cavity. If the walls are ~ 15° from vertical, a laser-feedback mechanism with the X or O mode can function

in principle, but it is unlikely that the cyclotron maser instability is the source of the energy because its growth rate is too low. Finally, it is significant that the timescales of the fine structure features often greatly exceed the inverse electron-neutral collision frequency, implying that features of individual batches of electrons would be isotropized by collisions on a timescale shorter than the observed features. In any case, only thermal electrons (of the order of 0.1 eV) have low enough parallel drift speeds to match the observed frequency drifts and frequency ranges of the wave features. It remains a theoretical challenge to explain these fine structure features of auroral roar emissions.

Acknowledgments. The authors acknowledge helpful discussions with A. T. Weatherwax and R. A. Treumann. S. G. Shepherd thanks the staff at the Churchill Northern Studies Centre for making his stay as comfortable as possible. This research was supported by National Science Foundation grant ATM-9316126 to Dartmouth College.

The Editor thanks T. J. Rosenberg and T. Oguti for their assistance in evaluating this paper.

References

Baumback, M. M., and W. Calvert, The minimum bandwidth of auroral kilometric radiation, *Geophys. Res. Lett.*, *14*, 119, 1987.

Calvert, W., A feedback model for the source of the auroral kilometric radiation, *J. Geophys. Res.*, *87*, 8199, 1982.

Doe, R. A., M. Mendillo, J. F. Vickrey, L. J. Zanetti, and R. W. Eastes, Observations of nightside auroral cavities, *J. Geophys. Res.*, *98*, 293, 1993.

Ellis, G. R. A., The Jupiter radio bursts, *Proc. Astron. Soc. Aust.*, *2*, 236, 1974.

Ellis, G. R. A., The source of the Jupiter *S*-bursts, *Nature*, *283*, 236, 1980.

Ellis, G. R. A., Observations of the Jupiter *S*-bursts between 3.2 and 32 MHz, *Aust. J. Phys.*, *35*, 165, 1982.

Gough, M. P., and A. Urban, Auroral beam/plasma interaction observed directly, *Planet. Space Sci.*, *31*, 875, 1983.

Gurnett, D. A., and R. R. Anderson, The kilometric radio emission spectrum: Relationship to auroral acceleration processes, in *Physics of Auroral Arc Formation, Geophys. Monogr. Ser.*, vol. 25, edited by S.-I. Akasofu and J. R. Kan, p. 341, AGU, Washington, D. C., 1981.

Kelley, M. C., *The Earth's Ionosphere: Plasma Physics and Electrodynamics*, Academic, San Diego, Calif., 1989.

Kellogg, P. J., and S. J. Monson, Radio emissions from the aurora, *Geophys. Res. Lett.*, *6*, 297, 1979.

Kellogg, P. J., and S. J. Monson, Further studies of auroral roar, *Radio Sci.*, *19*, 551, 1984.

LaBelle, J., Radio noise of auroral origin: 1968-1988, *J. Atmos. Terr. Phys.*, *51*, 197, 1989.

LaBelle, J., and A. T. Weatherwax, Ground-based observations of LF/MF/HF radio waves of auroral origin, in *Physics of Space Plasmas (1992)*, edited by T. Chang, p. 223, Scientific Publishers, Cambridge, Massachusetts, 1992.

LaBelle, J., M. L. Trimpi, R. Brittain, and A. T. Weatherwax, Fine structure of auroal roar emissions, *J. Geophys. Res.*, *100*, 21953, 1995.

Shepherd, S. G., J. LaBelle, and M. L. Trimpi, Polarization of auroral radio emissions, *Geophys. Res. Lett.*, *24*, 3161, 1997.

Warwick, J. W., et al., Voyager 1 planetary radio astronomy observations near Jupiter, *Science*, *204*, 995, 1979.

Weatherwax, A. T., Ground-based observations of auroral radio emissions, Ph.D. thesis, Dartmouth College, Hanover, N. H., 1994.

Weatherwax, A. T., J. LaBelle, M. L. Trimpi, and R. Brittain, Ground-based observations of radio emissions near $2f_{ce}$ and $3f_{ce}$ in the auroral zone, *Geophys. Res. Lett.*, *20*, 1447, 1993.

Weatherwax, A. T., J. LaBelle, M. L. Trimpi, R. A. Treumann, J. Minow, and C. Deehr, Statistical and case studies of radio emissions observed near $2f_{ce}$ and $3f_{ce}$ in the auroral zone, *J. Geophys. Res.*, *100*, 7745, 1995.

Yoon, P. H., A. T. Weatherwax, T. J. Rosenberg, and J. LaBelle, Lower ionospheric cyclotron maser theory: A possible source of $2f_{ce}$ and $3f_{ce}$ auroral radio emissions, *J. Geophys. Res.*, *101*, 27015, 1996.

Yoon, P. H., A. T. Weatherwax, and T. J. Rosenberg, On the generation of auroral radio emissions at harmonics of the lower ionospheric electron cyclotron frequency, *J. Geophys. Res.*, in press, 1998.

Zarka, P., T. Farges, B. P. Ryabov, M. Abada-Simon, and L. Denis, A scenario for Jovian *S* bursts, *Geophys. Res. Lett.*, *23*, 125, 1996.

J. LaBelle, S. G. Shepherd, and M. L. Trimpi, Department of Physics and Astronomy, Dartmouth College, Wilder Hall, Hinmann Box 6127, Hanover, NH 03755. (e-mail: jlabelle@einstein.dartmouth.edu; simon@einstein.dartmouth.edu; mike@einstein.dartmouth.edu)

(Received June 10, 1997; revised September 29, 1997; accepted October 28, 1997.)